

SUPPLEMENTARY INFORMATION

Details of DFT calculation of the PES

Our calculations use the NWChem software package version 6.5¹ implementing the CDFT algorithm of reference.² Although this version of the software only provides direct information on diabatic energies, local modifications of the software allowed calculation of adiabats.

As noted in the text, producing a physically reasonable PES required careful treatment of functionals, CDFT constraints, and outlying points. Due to the large size of the system, the use of long-range corrected functionals such as ω B97X-D^{3, 4} or CAM-B3LYP⁵⁻⁸ that are popular in treating organic semiconductors is computationally expensive. Instead, the less expensive B3LYP functional⁵⁻⁷ was used for geometry optimizations. B3LYP has been used in other CDFT work that effectively modeled charge transfer processes in organic semiconductors,^{2, 9-12} and is generally one of the most trusted functionals for geometry optimizations in DFT. However, when B3LYP was used for our single-point calculations, we found that the adiabats' minimum was at the halfway point of our reaction coordinate, suggesting that the electron delocalizes between the molecules without transport occurring. Although there may be significant delocalization in some PCBM materials, a PES that leads to a complete lack of transport is obviously in disagreement with the known charge transport properties of PCBM devices. Therefore, for the single-point calculations we utilized the Becke Half&Half functional,¹³ which is known to be effective for calculating couplings.¹⁴ The 6-31G* basis set, which has been applied successfully in previous CDFT work on organic molecules^{2, 10-12} was used. To improve the treatment of van der Waals effects, the dispersion correction of Grimme et al. was applied to the geometry optimizations.¹⁵ To maintain the spacing between fullerenes consistent with the PCBM crystal structure, one atom from each fullerene at the intermolecular interface was fixed in space during the optimizations.

In order to use the code available for the creation of adiabats in NWChem, it was necessary to allow the constrained charges to delocalize over the functional group as well as the C₆₀ cage. However, the diabats created with this constraint had a somewhat erratic shape (shown in Fig. S1), probably indicating that the reaction coordinate of Eq. 2 was a poor approximation for this constraint. To avoid problems caused by this spurious result, we utilized a reaction coordinate created from CDFT calculations in which the excess charge was constrained only to the C₆₀ cage of the molecule.

Our reaction coordinate was discretized into 21 points. We found that the diabats curled sharply upwards in energy in the last few points of the reaction coordinate, which resulted in erratic behavior of the adiabat in the last two points. This behavior is not surprising given our choice to use different functionals for the geometry optimizations and single-point calculations. Thus, we believe that these four ill-behaved points are not of any physical significance, and these points were discarded, leaving the 17-point PES as shown in Fig. 3 of the main text. A plot of the diabats without elimination of the four points is shown in Fig. S2. The omission of the four points increases the asymmetry of the diabatic and adiabatic PESs, lowering the energy of the final state relative to the initial state. As discussed in the text, asymmetric PESs should be common in OPVs; therefore, this asymmetry is not problematic for the present work.

Although various geometry optimization procedures may be useful to explore in future work, the variations in the PES of the magnitude that we discuss here are unlikely to affect our present conclusions. The sensitivity of the LMD model to variations in the PES can be estimated using Kramers' theory. For our system, we find that a doubling of the energy barrier E_B in the Kramers' rate equation leads to only a modest change in rate, with the rate reduced by a factor of ~ 0.4 . Thus, for the level of precision that we seek in this paper (in which even our experimental benchmark contains significant uncertainty), the uncertainty involved in our PES is not particularly concerning.

We note that the periodic boundary condition approach that we used to create an infinite PES leads to discontinuities in the first derivative at points A, B, C, etc. in Fig. 3b. Such discontinuities could be smoothed with a method such as a cubic spline interpolation if desired; however, within the LMD

propagation formalism that we discuss below, these discontinuities do not cause instability or significant error in the results.

Derivation of friction parameter γ_D

Here we apply the model of the damped harmonic oscillator to our m_{eff} and PES to obtain an estimate of γ_D . We use the harmonic oscillator equation of motion

$$\frac{d^2x}{dt^2} + 2\zeta \frac{dx}{dt} + \omega_0^2 x = 0 \quad (S1)$$

ζ is a friction parameter where $\zeta = \frac{\gamma}{2}$. At the crossover from over-damped to under-damped motion $\zeta = \omega_0$, where ω_0 is the natural frequency defined as $\sqrt{\frac{k}{m_{eff}}}$ for the harmonic oscillator and k is the bond force constant. From this we obtain the critical damping value $\gamma = 2\sqrt{\frac{k}{m_{eff}}}$. For the harmonic oscillator $\Delta U = \frac{1}{2}k\Delta x^2$ near the minimum, which we treat as the leftmost area of the PES shown in Fig. 3a. For this region of the PES $k \sim 0.04 \frac{eV}{\text{\AA}^2}$. Thus for a given value of m_{eff} , the order of magnitude of the friction is taken to be $\gamma_D \sim 2\sqrt{\frac{0.04}{m_{eff}}}$. To explore the region near the transition from under-damping to over-damping, we test several values of $\gamma = p\gamma_D$ with p values of 0.036, 0.36, and 3.6.

Numerical integration of the LMD

The fundamental equation for LMD of Eq. 1 is propagated from time t to $t + \Delta t$ according to the method of Ladd:¹⁶

$$= x_t + \frac{1}{2} v_t \Delta t$$

$$v_{t+\Delta t} = \frac{(1-\alpha^{(1)/2})v_t + m^{-1}F^{(1)}\Delta t + \sqrt{2m^{-1}k_B T \alpha^{(1)}}\phi_t}{(1+\alpha^{(1)/2})} \quad (S2)$$

$$x_{t+\Delta t} = x^{(1)} + \frac{1}{2} v_{t+\Delta t} \Delta t$$

We set the friction parameter to $\alpha^{(1)} = \gamma * dt$, where γ is the friction constant from Eq. 1. $m = m_{eff}$ and ϕ_t is a random number chosen at every time step to represent the random force R from Eq. 1. The force F is calculated numerically at each step as

$$F^{(1)} = -\frac{U(x^1+dx) - U(x^1-dx)}{2dx} \quad (S3)$$

where $dx = 0.0053 \text{\AA}$. We note that although the PES shown in Fig. 3b has discontinuities in the derivative at points A, B, C, etc., this algorithm is stable with respect to such discontinuities, with dx so small that cases in which $F^{(1)}$ involves a crossing over a discontinuity is an infrequent and insignificant event. All simulations are conducted with a time step of 20 fs. The time length of the simulations t_{max}

was chosen based on the values of m_{eff} and γ , using trial and error to find simulation lengths that allowed all 500 runs to achieve transfer.

Supplementary Information Figures

Fig. S1. Diabatic PESs derived from CDFT runs in which the excess charge was constrained both the fullerene and its functional group. These PESs are a function of reaction coordinate rather than space. The x -axis shows the value of the interpolation parameter q of Eq. 2 that is used to derive the reaction coordinate. Because the shape of these surfaces was somewhat erratic (probably evidence that the reaction coordinate was a poor approximation for this constraint), the reaction coordinate that was employed in the LMD simulations was derived from CDFT calculations constraining the excess charge to C_{60} only.

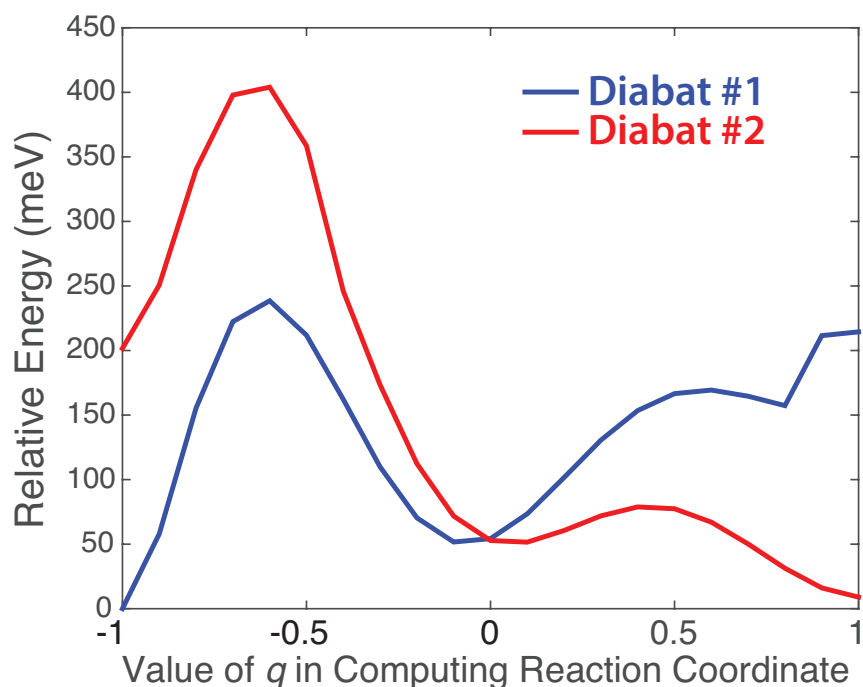
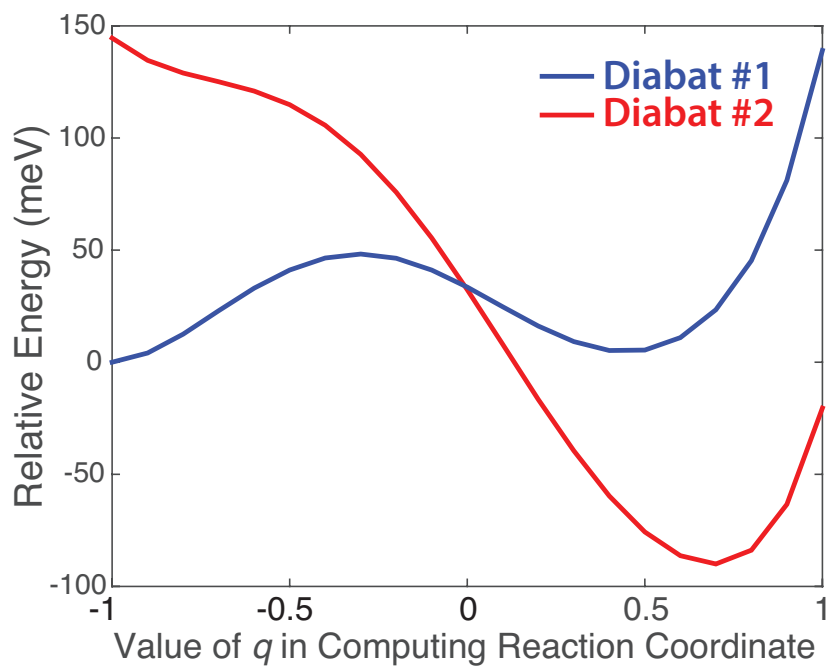


Fig. S2. Diabatic PESs obtained when all 21 points of the reaction coordinate were included. These PESs are a function of reaction coordinate rather than space. The x -axis shows the value of the interpolation parameter q of Eq. 2 that is used to derive the reaction coordinate. Because of the rise in energies at the end, which we attribute to the difference in the DFT functional between the geometry optimizations and single-point calculations, the final four points were omitted from the PES used in the simulations.



References

1. M. Valiev, E. J. Bylaska, N. Govind, K. Kowalski, T. P. Straatsma, H. J. J. v. Dam, D. Wang, J. Nieplocha, E. Apra, T. L. Windus and W. A. d. Jong, *Comput. Phys. Commun.*, 2010, **181**, 1477-1489.
2. Q. Wu and T. V. Voorhis, *Phys. Rev. A*, 2005, **72**, 024502.
3. J.-D. Chai and M. Head-Gordon, *J. Chem. Phys.*, 2008, **128**, 084106.
4. J.-D. Chai and M. Head-Gordon, *Phys. Chem. Chem. Phys.*, 2008, **10**, 6615-6620.
5. S. H. Vosko, L. Wilk and M. Nusair, *Can. J. Phys.*, 1980, **58**, 1200-1211.
6. B. Miehlich, A. Savin, H. Stoll and H. Preuss, *Chem. Phys. Lett.*, 1989, **157**, 200-206.
7. C. Lee, W. Yang and R. G. Parr, *Phys. Rev. B*, 1988, **37**, 785-789.
8. T. Yanai, D. P. Tew and N. C. Handy, *Chem. Phys. Lett.*, 2004, **393**, 51-57.
9. S. Difley and T. V. Voorhis, *J. Chem. Theory Comput.*, 2011, **7**, 594-601.
10. T. V. Voorhis, T. Kowalczyk, B. Kaduk, L.-P. Wang, C.-L. Cheng and Q. Wu, *Annu. Rev. Phys. Chem.*, 2010, **61**, 149-170.
11. Q. Wu and T. V. Voorhis, *J. Chem. Phys.*, 2006, **125**, 164105.
12. Q. Wu and T. V. Voorhis, *J. Phys. Chem. A*, 2006, **110**, 9212.
13. A. D. Becke, *J. Chem. Phys.*, 1993, **98**, 1372-1377.
14. A. Kubas, F. Hoffmann, A. Heck, H. Oberhofer, M. Eistner and J. Blumberger, *J. Chem. Phys.*, 2014, **140**, 104105.
15. S. Grimme, *J. Comput. Chem.*, 2006, **27**, 1787-1799.
16. A. J. C. Ladd, Kazimierz, Poland, 2009.
1. M. Valiev, E. J. Bylaska, N. Govind, K. Kowalski, T. P. Straatsma, H. J. J. v. Dam, D. Wang, J. Nieplocha, E. Apra, T. L. Windus and W. A. d. Jong, *Comput. Phys. Commun.*, 2010, **181**, 1477-1489.
2. Q. Wu and T. V. Voorhis, *Phys. Rev. A*, 2005, **72**, 024502.
3. J.-D. Chai and M. Head-Gordon, *J. Chem. Phys.*, 2008, **128**, 084106.
4. J.-D. Chai and M. Head-Gordon, *Phys. Chem. Chem. Phys.*, 2008, **10**, 6615-6620.
5. S. H. Vosko, L. Wilk and M. Nusair, *Can. J. Phys.*, 1980, **58**, 1200-1211.
6. B. Miehlich, A. Savin, H. Stoll and H. Preuss, *Chem. Phys. Lett.*, 1989, **157**, 200-206.
7. C. Lee, W. Yang and R. G. Parr, *Phys. Rev. B*, 1988, **37**, 785-789.
8. T. Yanai, D. P. Tew and N. C. Handy, *Chem. Phys. Lett.*, 2004, **393**, 51-57.
9. S. Difley and T. V. Voorhis, *J. Chem. Theory Comput.*, 2011, **7**, 594-601.
10. T. V. Voorhis, T. Kowalczyk, B. Kaduk, L.-P. Wang, C.-L. Cheng and Q. Wu, *Annu. Rev. Phys. Chem.*, 2010, **61**, 149-170.
11. Q. Wu and T. V. Voorhis, *J. Chem. Phys.*, 2006, **125**, 164105.
12. Q. Wu and T. V. Voorhis, *J. Phys. Chem. A*, 2006, **110**, 9212.
13. A. D. Becke, *J. Chem. Phys.*, 1993, **98**, 1372-1377.
14. A. Kubas, F. Hoffmann, A. Heck, H. Oberhofer, M. Eistner and J. Blumberger, *J. Chem. Phys.*, 2014, **140**, 104105.
15. S. Grimme, *J. Comput. Chem.*, 2006, **27**, 1787-1799.
16. A. J. C. Ladd, Kazimierz, Poland, 2009.